
An Expectation-Maximization Perspective on Federated Learning

Christos Louizos[‡], Matthias Reisser[‡], Joseph Soriaga[‡], Max Welling[†]
[‡]Qualcomm AI Research *, [†]University of Amsterdam
{clouizos,mreisser,jsoriaga}@qti.qualcomm.com, m.welling@uva.nl

Abstract

Federated learning describes the distributed training of models across multiple clients while keeping the data private on-device. In this work, we view the server-orchestrated federated learning process as a hierarchical latent variable model where the server provides the parameters of a prior distribution over the client-specific model parameters. We show that with simple Gaussian priors and a *hard* version of the well known Expectation-Maximization (EM) algorithm, learning in such a model corresponds to FedAvg, the most popular algorithm for the federated learning setting. This perspective on FedAvg unifies several recent works in the field and opens up the possibility for extensions through different choices for the hierarchical model. Based on this view, we further propose a variant of the hierarchical model that employs prior distributions to promote sparsity. By similarly using the hard-EM algorithm for learning, we obtain FedSparse, a procedure that can learn sparse neural networks in the federated learning setting. FedSparse reduces communication costs from client to server and vice-versa, as well as the computational costs for inference with the sparsified network – both of which are of great practical importance in federated learning.

1 Introduction

Smart devices have become ubiquitous in today’s world and are generating large amounts of potentially sensitive data. Traditionally, such data is transmitted and stored in a central location for training machine learning models. Such methods rightly raise privacy concerns, and we seek the means for training powerful models, such as neural networks, without the need to transmit potentially sensitive data. To this end, Federated Learning (FL) [22] has been proposed to train global machine learning models without the need for participating devices to transmit their data to the server. The Federated Averaging (FedAvg) [22] algorithm communicates the parameters of the machine learning model instead of the data itself, which is a more private means of communication.

In this work, we adopt a perspective on server-orchestrated federated learning through the lens of a simple hierarchical latent variable model; the server provides the parameters of a prior distribution over the client-specific neural network parameters, which are subsequently used to “explain” the client-specific dataset. A visualization of this graphical model can be seen in Figure 1. We show that when the server provides a Gaussian prior over these parameters, learning with the *hard* version of the Expectation-Maximization (EM) algorithm will yield the FedAvg procedure. This view of FedAvg has several interesting consequences, as it connects several recent works in federated learning and bridges FedAvg with meta-learning.

Furthermore, this view of federated learning provides a good basis for developing several extensions to the vanilla FedAvg algorithm by appropriately changing the hierarchical model. Through this perspective, we develop FedSparse by extending the graphical model to the one in Figure 2.

*Qualcomm AI Research is an initiative of Qualcomm Technologies, Inc. and/or its subsidiaries.

FedSparse allows for learning sparse neural network models at the client and server via a careful choice of the priors within the hierarchical model.

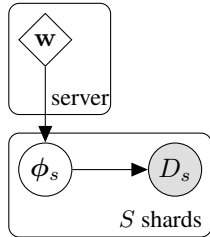


Figure 1: The simple hierarchical model for server-orchestrated federated learning. With a Gaussian prior for the local parameters ϕ_s centered at the server parameters w and hard-EM for learning we obtain FedAvg.

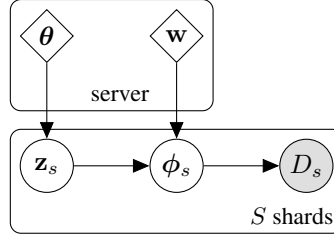


Figure 2: Modifying the hierarchical model to allow for sparsity in the local parameters ϕ_s with the spike and slab distribution [23]. The server parameter θ governs a Bernoulli prior distribution over the local variables z_s , the value of which determine whether a parameter in ϕ_s is active or not. When a parameter is active, the prior is a Gaussian centered at the server parameters w . By using hard-EM on this variant of the hierarchical model, we obtain FedSparse.

Sparse neural networks are appealing for the FL scenario, especially in the “cross-device” setting [14], as they can tackle several practical challenges. In particular, communicating model updates over multiple rounds across many devices can incur significant communication costs. Communication via the public internet infrastructure and mobile networks is potentially slow and not for free. Equally important, training (and inference) takes place on-device and is therefore restricted by the edge devices’ hardware constraints on memory, speed and heat dissipation capabilities. Therefore, FedSparse provides models that tackle both of the challenges mentioned above since they can simultaneously reduce the overall communication and computation at the client devices. Addressing these challenges is an important step towards building practical FL systems, as also discussed in [14]. Empirically, we see that FedSparse provides better communication-accuracy trade-offs compared to, FedAvg, prior works that similarly target joint reductions of computation and communication costs [5], as well as another baseline that uses L_1 regularization at the client level (for pruning) and standard parameter averaging at the server level.

2 A hierarchical model interpretation of federated learning

The server-orchestrated variant of federated learning is mainly realized via the FedAvg [22] algorithm, which is a simple iterative procedure consisting of four simple steps. At the beginning of each round t , the server communicates the model parameters, let them be w , to a subset of the devices. The devices then proceed to optimize w , *e.g.*, via stochastic gradient descent, on their respective dataset via a given loss function

$$\mathcal{L}_s(\mathcal{D}_s, w) := \frac{1}{N_s} \sum_{i=1}^{N_s} L(\mathcal{D}_{si}, w) \quad (1)$$

where s indexes the device, \mathcal{D}_s corresponds to the dataset at device s and N_s corresponds to its size. After a specific amount of epochs of optimization on \mathcal{L}_s is performed, denoted as E , the devices communicate the current state of their parameters, let it be ϕ_s , to the server. The server then performs an update to its own model by simply averaging the client specific parameters $w_t = \frac{1}{S} \sum_s \phi_s$.

2.1 FedAvg as learning in a hierarchical model

We now ask the following question; does the FedAvg algorithm correspond to learning on a specific model? Let us consider the following objective function:

$$\arg \max_w \sum_{s=1}^S \log p(\mathcal{D}_s | w), \quad (2)$$

where \mathcal{D}_s corresponds to the shard specific dataset that has N_s datapoints, $p(\mathcal{D}_s|\mathbf{w})$ corresponds to the likelihood of \mathcal{D}_s under the server parameters \mathbf{w} . Now consider decomposing each of the shard specific likelihoods as follows:

$$p(\mathcal{D}_s|\mathbf{w}) = \int p(\mathcal{D}_s|\phi_s)p(\phi_s|\mathbf{w})d\phi_s, \quad p(\phi_s|\mathbf{w}) = \frac{1}{Z} \exp\left(-\frac{\lambda}{2}\|\phi_s - \mathbf{w}\|^2\right), \quad (3)$$

where we introduced the auxiliary latent variables ϕ_s , which are the parameters of the local model at shard s . The server parameters \mathbf{w} act as the center for the Gaussian prior at Eq. 3 over the shard specific parameters with the precision λ acting as a regularization strength that prevents ϕ_s from moving too far from \mathbf{w} . By putting everything together, the total objective will be

$$\mathcal{F}(\mathbf{w}) := \sum_s \log \int p(\mathcal{D}_s|\phi_s) \frac{\exp\left(-\frac{\lambda}{2}\|\phi_s - \mathbf{w}\|^2\right)}{Z} d\phi_s, \quad (4)$$

and the graphical model of this process can be seen at Figure 1.

How can we then optimize Eq. 4 in the presence of these latent variables ϕ_s ? The traditional way to optimize such objectives is through Expectation-Maximization (EM). EM consists of two steps, the E-step where we form the posterior distribution over these latent variables

$$p(\phi_s|\mathcal{D}_s, \mathbf{w}) = \frac{p(\mathcal{D}_s|\phi_s)p(\phi_s|\mathbf{w})}{p(\mathcal{D}_s|\mathbf{w})}, \quad (5)$$

and the M-step where we maximize the probability of \mathcal{D}_s w.r.t. the parameters of the model \mathbf{w} by marginalizing over this posterior

$$\arg \max_{\mathbf{w}} \sum_s \mathbb{E}_{p(\phi_s|\mathcal{D}_s, \mathbf{w}_{\text{old}})}[\log p(\mathcal{D}_s, \phi_s|\mathbf{w})] = \arg \max_{\mathbf{w}} \sum_s \mathbb{E}_{p(\phi_s|\mathcal{D}_s, \mathbf{w}_{\text{old}})}[\log p(\phi_s|\mathbf{w})]. \quad (6)$$

If we perform a single gradient step for \mathbf{w} in the M-step, this procedure corresponds to doing gradient ascent on the original objective at Eq. 4, a fact we show in Appendix F.

When posterior inference is intractable, hard-EM is usually employed as a simpler alternative. In this case we make ‘‘hard’’ assignment for the latent variables ϕ_s in the E-step by approximating $p(\phi_s|\mathcal{D}_s, \mathbf{w})$ with its most probable point, *i.e.*

$$\phi_s^* = \arg \max_{\phi_s} \frac{p(\mathcal{D}_s|\phi_s)p(\phi_s|\mathbf{w})}{p(\mathcal{D}_s|\mathbf{w})} = \arg \max_{\phi_s} \log p(\mathcal{D}_s|\phi_s) + \log p(\phi_s|\mathbf{w}). \quad (7)$$

This is usually easier to do as we can use techniques such as stochastic gradient ascent. Given these hard assignments, the M-step then corresponds to another simple maximization

$$\arg \max_{\mathbf{w}} \frac{1}{S} \sum_s \log p(\phi_s^*|\mathbf{w}). \quad (8)$$

As a result, performing hard-EM on the objective of Eq. 4 corresponds to a block coordinate ascent type of algorithm on the following objective function

$$\arg \max_{\phi_{1:S}, \mathbf{w}} \sum_s (\log p(\mathcal{D}_s|\phi_s) + \log p(\phi_s|\mathbf{w})), \quad (9)$$

where we alternate between optimizing $\phi_{1:S}$ and \mathbf{w} while keeping the other fixed.

How does this learning procedure correspond to FedAvg? By letting $\lambda \rightarrow 0$ in Eq. 3 it is clear that the hard assignments in the E-step mimic the process of optimizing a local model on the data of each shard. In fact, even by optimizing the model locally with stochastic gradient ascent for a fixed number of iterations with a given learning rate, we implicitly assume a specific prior over the parameters; for linear regression, this prior is a Gaussian centered at the initial value of the parameters [29] whereas for non-linear models it bounds the distance from the initial point. After obtaining ϕ_s^* the M-step then corresponds to

$$\arg \max_{\mathbf{w}} \mathcal{L}_r := \sum_s -\frac{\lambda}{2}\|\phi_s^* - \mathbf{w}\|^2 + C, \quad (10)$$

and we can easily find a closed form solution by setting the derivative of the objective w.r.t. \mathbf{w} to zero and solving for \mathbf{w} :

$$\frac{\partial \mathcal{L}_r}{\partial \mathbf{w}} = 0 \Rightarrow \lambda \sum_s (\phi_s^* - \mathbf{w}) = 0 \Rightarrow \mathbf{w} = \frac{1}{S} \sum_s \phi_s^*. \quad (11)$$

It is easy to see that the optimal solution for \mathbf{w} given $\phi_{1:S}^*$ is the same as the one from FedAvg. Notice that for the ‘‘cross-device’’ settings of FL, the sum over all of the shards in the objective can be expensive. Nevertheless, it can easily be approximated by selecting a subset of the shards B , i.e., $\mathcal{L}_r \approx \frac{S}{B} \sum_{s \in B} -\frac{\lambda}{2} \|\phi_s^* - \mathbf{w}\|^2 + C$. In this way, we only have to estimate ϕ_s^* for the selected shards since the averaging for \mathbf{w} involves only the selected shards.

Of course, FedAvg does not optimize the local parameters ϕ_s to convergence at each round, so one might wonder whether this correspondence is still valid. It turns out that the alternating procedure of EM corresponds to block coordinate ascent on a single objective function, the variational lower bound of the marginal log-likelihood [24] of a given model. More specifically for our setting, we can see that the EM iterations perform block coordinate ascent on:

$$\sum_s \mathbb{E}_{q_{\mathbf{w}_s}(\phi_s)} [\log p(\mathcal{D}_s | \phi_s) + \log p(\phi_s | \mathbf{w})] + H[q_{\mathbf{w}_s}(\phi_s)] \quad (12)$$

to optimize $\mathbf{w}_{1:S}$ and \mathbf{w} , where \mathbf{w}_s are the parameters of the variational approximation to the posterior distribution $p(\phi_s | \mathcal{D}_s, \mathbf{w})$ and $H[q]$ corresponds to the entropy of the q distribution. To obtain the hard-EM procedure, and thus FedAvg, we can use a (numerically) deterministic distribution for ϕ_s , $q_{\mathbf{w}_s}(\phi_s) := \mathcal{N}(\mathbf{w}_s, \epsilon \mathbf{I})$. This leads us to the same objective as in Eq. 9, since the expectation concentrates on a single term and the entropy of $q_{\mathbf{w}_s}(\phi_s)$ becomes a constant independent of the optimization. In this case, the optimized value for ϕ_s after a fixed number of steps corresponds to the \mathbf{w}_s of the variational approximation.

It is interesting to contrast recent literature under the lens of this procedure. Optimizing the same model with hard-EM but with a non-trivial λ results in the same procedure that was proposed by [18]. Furthermore, using the difference of the local parameters to the global parameters as a ‘‘gradient’’ [28] is equivalent to hard-EM on the same model, where in the M-step, instead of a closed-form update, we take a single gradient step and absorb the scaling λ in the learning rate. In addition, this view makes precise the idea that FedAvg is a meta-learning algorithm [13]; the underlying hierarchical model it optimizes is similar to the ones used in meta-learning [10, 6].

Besides connecting recent work in FL, this view also serves as a good basis for new algorithms for federated learning. The most straightforward way is to use an alternative prior in the hierarchical model, resulting in different local training and server-side updating behaviors. For example, one could use a Laplace prior, $p(\phi_s | \mathbf{w}) = \text{Lap}(\mathbf{w}, \frac{1}{\lambda})$, which would result into the server selecting the median instead of averaging, or a mixture of Gaussians prior, $p(\phi_s | \mathbf{w}_{1:K}, \frac{1}{\lambda}) = \frac{1}{K} \sum_k \mathcal{N}(\mathbf{w}_k, \frac{1}{\lambda})$, which would result into training an ensemble of models at the server. We provide the details in Appendix J. In this work, we focus on tackling the communication and computational costs of FL, which is important and highly beneficial for practical applications of ‘‘cross-device’’ FL [14]. For this reason, we replace the Gaussian prior with a sparsity inducing prior, namely the spike and slab prior [23]. We describe the resulting algorithm, FedSparse, in the next section.

3 The FedSparse algorithm: sparsity in federated learning

Encouraging sparsity in FL has two main advantages; the model becomes smaller, thus less resource-intensive to evaluate, and it cuts down on communication costs as the pruned parameters do not need to be communicated. The golden standard for sparsity in probabilistic models is the spike and slab [23] prior. It is a mixture of two components, a delta spike at zero, $\delta(0)$, and a continuous distribution over the real line, *i.e.* the slab. More specifically, by adopting a Gaussian slab for each local parameter ϕ_{si} we have that

$$p(\phi_{si} | \theta_i, \mathbf{w}_i) = (1 - \theta_i) \delta(0) + \theta_i \mathcal{N}(\phi_{si} | \mathbf{w}_i, 1/\lambda), \quad (13)$$

or equivalently as a hierarchical model

$$p(\mathbf{z}_{si}) = \text{Bern}(\theta_i), \quad p(\phi_{si} | \mathbf{z}_{si} = 1, \mathbf{w}_i) = \mathcal{N}(\phi_{si} | \mathbf{w}_i, 1/\lambda), \quad p(\phi_{si} | \mathbf{z}_{si} = 0) = \delta(0) \quad (14)$$

$$p(\phi_{si} | \theta_i, \mathbf{w}_i) = \sum_{\mathbf{z}_{si}} p(\mathbf{z}_{si} | \theta_i) p(\phi_{si} | \mathbf{z}_{si}, \mathbf{w}_i), \quad (15)$$

where \mathbf{z}_{si} plays the role of a ‘‘gating’’ variable that switches on or off the parameter ϕ_{si} . We thus modify the hierarchical model at Figure 1 to use this new prior. The resulting hierarchical model can be seen in Figure 2, where \mathbf{w} , $\boldsymbol{\theta}$ will be the server-side model weights and probabilities of the binary gates.

Following the FedAvg paradigm of simple point estimation, we will use hard-EM in order to optimize \mathbf{w} , $\boldsymbol{\theta}$. By using approximate distributions $q_{\mathbf{w}_s}(\phi_s|\mathbf{z}_s)$, $q_{\pi_s}(\mathbf{z}_s)$, the variational lower bound for this model becomes

$$\sum_s \mathbb{E}_{q_{\pi_s, \mathbf{w}_s}(\mathbf{z}_s, \phi_s)} [\log p(\mathcal{D}_s|\phi_s) + \log p(\phi_s, \mathbf{z}_s|\mathbf{w}, \boldsymbol{\theta}) - \log q_{\mathbf{w}_s}(\phi_s|\mathbf{z}_s)] + H[q_{\pi_s}(\mathbf{z}_s)], \quad (16)$$

which is to be optimized with respect to $\mathbf{w}_{1:S}$, \mathbf{w} , $\pi_{1:S}$, $\boldsymbol{\theta}$. For the shard specific weight distributions, as they are continuous, we will use $q_{\mathbf{w}_s}(\phi_{si}|\mathbf{z}_{si} = 1) := \mathcal{N}(\mathbf{w}_{si}, \epsilon)$, $q(\phi_{si}|\mathbf{z}_{si} = 1) := \mathcal{N}(0, \epsilon)$ with $\epsilon \approx 0$ which will be, numerically speaking, deterministic. For the gating variables, as they are binary, we will use $q_{\pi_{si}}(\mathbf{z}_{si}) := \text{Bern}(\pi_{si})$ with π_{si} being the probability of activating local gate \mathbf{z}_{si} . In order to do hard-EM for the binary variables, we will remove the entropy term for the $q_{\pi_s}(\mathbf{z}_s)$ from the aforementioned bound as this will encourage the approximate distribution to move towards the most probable value for \mathbf{z}_s . Furthermore, by relaxing the spike at zero to a Gaussian with precision λ_2 , *i.e.*, $p(\phi_{si}|\mathbf{z}_{si} = 0) = \mathcal{N}(0, 1/\lambda_2)$, and by plugging in the appropriate expressions into Eq. 16 we can show that the local and global objectives will be

$$\begin{aligned} \mathcal{L}_s(\mathcal{D}_s, \mathbf{w}, \boldsymbol{\theta}, \mathbf{w}_s, \pi_s) &:= C + \mathbb{E}_{q_{\pi_s}(\mathbf{z}_s)} \left[\sum_i^{N_s} L(\mathcal{D}_{si}, \mathbf{w}_s \odot \mathbf{z}_s) \right] - \frac{\lambda}{2} \sum_j \pi_{sj} (\mathbf{w}_{sj} - \mathbf{w}_j)^2 \\ &\quad - \lambda_0 \sum_j \pi_{sj} + \sum_j (\pi_{sj} \log \theta_j + (1 - \pi_{sj}) \log(1 - \theta_j)), \end{aligned} \quad (17)$$

$$\mathcal{L} := \sum_{s=1}^S \mathcal{L}_s(\mathcal{D}_s, \mathbf{w}, \boldsymbol{\theta}, \mathbf{w}_s, \pi_s) \quad (18)$$

respectively, where $\lambda_0 = \frac{1}{2} \log \frac{\lambda_2}{\lambda}$ and C is a constant independent of the variables to be optimized. The derivation can be found in Appendix G. It is interesting to see that the final objective at each shard intuitively tries to find a trade-off between four things: 1) explaining the local dataset \mathcal{D}_s , 2) having the local weights close to the server weights (regulated by λ), 3) having the local gate probabilities close to the server probabilities and 4) reducing the local gate activation probabilities to prune away a parameter (regulated by λ_0). The latter is an L_0 regularization term, akin to the one proposed by [21].

Now let us consider what happens at the server after the local shard, through some procedure, optimized \mathbf{w}_s and π_s . Since the server loss for \mathbf{w} , $\boldsymbol{\theta}$ is the sum of all local losses, the gradient for each of the parameters will be

$$\frac{\partial \mathcal{L}}{\partial \mathbf{w}} = \sum_s \lambda \pi_s (\mathbf{w}_s - \mathbf{w}), \quad \frac{\partial \mathcal{L}}{\partial \boldsymbol{\theta}} = \sum_s \left(\frac{\pi_s}{\boldsymbol{\theta}} - \frac{1 - \pi_s}{1 - \boldsymbol{\theta}} \right). \quad (19)$$

Setting these derivatives to zero, we see that the stationary points are

$$\mathbf{w} = \frac{1}{\sum_j \pi_j} \sum_s \pi_s \mathbf{w}_s, \quad \boldsymbol{\theta} = \frac{1}{S} \sum_s \pi_s \quad (20)$$

i.e., a weighted average of the local weights and an average of the local probabilities of keeping these weights. Therefore, since the π_s are being optimized to be sparse through the L_0 penalty, the server probabilities $\boldsymbol{\theta}$ will also become small for the weights that are used by only a small fraction of the shards. As a result, to obtain the final sparse architecture, we can prune the weights whose corresponding, learned, server inclusion probabilities $\boldsymbol{\theta}$ are less than a threshold, *e.g.*, 0.1. It should again be noted that the sums and averages of Eq. 19, 20 respectively can be easily approximated by subsampling a small set of clients S' from S . Therefore we do not have to consider all of the clients at each round, which would be prohibitive for ‘‘cross-device’’ FL.

3.1 Reducing the communication cost

The framework described so far allows us to learn a more efficient model. We now discuss how we can use it in order to cut down both download and upload communication costs during training.

Reducing client to server communication cost In order to reduce the client to server cost, we will communicate sparse samples from the local distributions instead of the distributions themselves; in this way, we do not have to communicate the zero values of the parameter vector, which leads to large savings. More specifically, we can express the gradients and stationary points for the server weights and probabilities as follows

$$\frac{\partial \mathcal{L}}{\partial \mathbf{w}} = \sum_s \lambda \mathbb{E}_{q_{\pi_s}(\mathbf{z}_s)} [\mathbf{z}_s (\mathbf{w}_s - \mathbf{w})], \quad \mathbf{w} = \mathbb{E}_{q_{\pi_{1:S}}(\mathbf{z}_{1:S})} \left[\frac{1}{\sum_j \mathbf{z}_j} \sum_s \mathbf{z}_s \mathbf{w}_s \right], \quad (21)$$

$$\frac{\partial \mathcal{L}}{\partial \boldsymbol{\theta}} = \sum_s \mathbb{E}_{q_{\pi_s}(\mathbf{z}_s)} \left[\frac{\mathbf{z}_s}{\boldsymbol{\theta}} - \frac{1 - \mathbf{z}_s}{1 - \boldsymbol{\theta}} \right], \quad \boldsymbol{\theta} = \frac{1}{S} \sum_s \mathbb{E}_{q_{\pi_s}(\mathbf{z}_s)} [\mathbf{z}_s]. \quad (22)$$

As a result, we can then communicate from the client only the subset of the local weights $\hat{\mathbf{w}}_s$ that are non-zero in $\mathbf{z}_s \sim q_{\pi_s}(\mathbf{z}_s)$, $\hat{\mathbf{w}}_s = \mathbf{w}_s \odot \mathbf{z}_s$, along with the \mathbf{z}_s . Having access to those samples, the server can then form 1-sample stochastic estimates of either the gradients or the stationary points for $\mathbf{w}, \boldsymbol{\theta}$. Notice that this is a way to reduce communication without adding bias in the gradients of the original objective. In case that we are willing to incur extra bias, future work can consider techniques such as quantization [2] and top-k gradient selection [20] to reduce communication even further.

Reducing the server to client communication cost The server needs to communicate to the clients the updated distributions at each round. Unfortunately, for simple unstructured pruning, this doubles the communication cost as for each weight \mathbf{w}_i there is an associated θ_i that needs to be sent to the client. To mitigate this effect, we will employ structured pruning, which introduces a single additional parameter for each group of weights. For groups of moderate sizes, *e.g.*, the set of weights of a given convolutional filter, the extra overhead is small. We can also take the communication cost reductions one step further if we allow for some bias in the optimization procedure; we can prune the global model during training after every round and thus send to each of the clients only the subset of the model that has survived. Notice that this is easy to do and does not require any data at the server. The inclusion probabilities $\boldsymbol{\theta}$ are available at the server, so we can remove the parameters that have θ less than a threshold, *e.g.* 0.1. This can lead to large reductions in communication costs, especially once the model becomes sufficiently sparse.

3.2 FedSparse in practice

Local optimization While optimizing for \mathbf{w}_s locally is straightforward to do with gradient-based optimizers, π_s is more tricky, as the expectation over the binary variables \mathbf{z}_s in Eq. 17 is intractable to compute in closed form and using Monte-Carlo integration does not yield reparametrizable samples. To circumvent these issues, we rewrite the objective in an equivalent form and use the hard-concrete relaxation from [21], which can allow for the straightforward application of gradient ascent. We provide the details in Appendix H. When the client has to communicate to the server, we propose to form $\hat{\mathbf{w}}_s$ by sampling from the zero-temperature relaxation, which yields exact binary samples. Furthermore, at the beginning of each round, following the practice of FedAvg, the participating clients initialize their approximate posteriors to be equal to the priors that were communicated from the server. Empirically, we found that this resulted in better global model accuracy.

Parameterization of the probabilities There is evidence that such optimization-based pruning can be inferior to simple magnitude-based pruning [9]. We, therefore, take an approach that combines the two and reminisces the recent work of [3]. We parameterize the probabilities $\boldsymbol{\theta}, \pi_s$ as a function of the model weights and magnitude-based thresholds that regulate how active a parameter can be:

$$\theta_g := \sigma \left(\frac{\|\mathbf{w}_g\|_2 - \tau_g}{T} \right), \quad \pi_{sg} := \sigma \left(\frac{\|\mathbf{w}_{sg}\|_2 - \tau_{sg}}{T} \right), \quad (23)$$

where the subscript g denotes the group, $\sigma(\cdot)$ is the sigmoid function, τ_g, τ_{sg} are the global and client specific thresholds for a given group g and T is a temperature hyperparameter. Following [3] we also “detach” the gradient of the weights through $\boldsymbol{\theta}, \pi_s$, to avoid decreasing the probabilities by just shrinking the weights. With this parametrization we lose the ability to get a closed form solution for the server thresholds, but nonetheless we can still perform gradient based optimization at the server by using the chain rule. For a positive threshold, we use a parametrization in terms of a softplus function, *i.e.*, $\tau = \log(1 + \exp(\mathbf{v}))$ where \mathbf{v} is the learnable parameter. The FedSparse algorithm is described in Alg. 1, 2 in the Appendix.

4 Related work

FedProx [18] adds a proximal term to the local objective at each shard, so that it prevents the local models from drifting too far from the global model, while still averaging the parameters at the server. In Section 2 we showed how such a procedure arises if we use a non-trivial precision for the Gaussian prior over the local parameters of the hierarchical model and apply hard-EM. Furthermore, FedAvg has been advocated to be a meta-learning algorithm in [13]; with our perspective, this claim is precise and shows that the underlying hierarchical model that FedAvg optimizes is the same as the models used in several meta-learning works [10, 6]. Furthermore, by performing a single gradient step for the M-step in the context of hard-EM applied at the model of Section 2, we see that we arrive at a procedure that has been previously explored both in a meta-learning context with the Reptile algorithm [25], as well as the federated learning context with the “generalized” FedAvg [28]. One important difference between meta-learning and FedAvg is that the latter maximizes the sum, across shards, marginal-likelihood in order to update the global parameters, whereas meta-learning methods usually optimize the global parameters such that the finetuned model performs well on the local validation sets. Exploring such parameter estimation methods, as, *e.g.*, in [6], in the federated scenario and how these relate to existing approaches that merge meta-learning with federated learning, *e.g.* [8], is an interesting avenue for future work. Finally, our EM perspective also applies to optimization works that improve model performance via model replicas [36, 27].

Adopting a hierarchical model perspective for federated learning is not new and has been explored previously in, *e.g.*, [34, 35, 7, 1]. [34, 35] consider the local parameters as “given” and then fit a prior model to uncover latent structure. This is only a part of our story; from our EM perspective, the *prior affects the local optimization itself*, thus it allows us to, *e.g.*, sparsify a neural network locally with FedSparse. [7, 1] are more similar to our work; they are both FedAvg-like procedures that can be viewed as a way to *aggregate inferences* across clients in order to get a “global” posterior approximation (albeit with different procedures) to the parameters of the server model. This is different to our view of FedAvg as learning the parameters of a *shared prior*, where the server provides the parameters for this prior, across clients. We believe that these views are complimentary to ours and combining the two is an interesting direction that we leave for future work.

Reducing communication costs is a well-known and explored topic in federated learning. FedSparse has close connections to federated dropout [5], as the latter can be understood via a similar hierarchical model, where gates \mathbf{z} are global and have a fixed probability θ for both the prior and the approximate posterior. Compared to federated dropout, FedSparse allows us to optimize the dropout rates to the data, such that they satisfy a given accuracy / sparsity trade-off, dictated by the hyperparameter λ_0 . Another benefit of our EM perspective is that it clarifies that the server can perform gradient-based optimization. As a result, we can harvest the large literature on efficient distributed optimization [20, 4, 31, 33], which involves gradient quantization, sparsification, and more general compression. On this front, there have also been other works that aim to reduce the communication cost in FL via such approaches [30, 11]. In general, such approaches can be orthogonal to FedSparse and exploring how they can be incorporated is a promising avenue for future research. Besides parameter / gradient compression, there are also works that reduce communication costs via other means. [15] reduces the number of training rounds necessary via a better optimization procedure and [19] reduces the amount of gradient queries by reusing gradients from previous iterations. Both of these are orthogonal to FedSparse, which decreases communication costs by reducing the number of parameters to transmit. Therefore, they could be combined for even more savings. As an example, we provide an experiment in Appendix E where we show the benefits of combining FedSparse with [15].

5 Experiments

We verify in three tasks whether FedSparse leads to similar or better global models compared to FedAvg while providing reductions in communication costs and efficient models. We include two baselines that also reduce communication costs by sparsifying the model; for the first, we consider the federated dropout procedure from [5], which we refer to as FedDrop, and for the second, we implement a variant of FedAvg where the clients locally perform group L_1 regularization [32] in order to sparsify their copy of the model. The latter, which we refer to as FedL1, is closer to what we do in FedSparse and can similarly reduce the communication costs by employing a soft thresholding step on the model before communicating. For each task, we present the results for FedSparse with

regularization strengths that target three sparsity levels: low, mid, and high. For the FedDrop baseline, we experiment with multiple combinations of dropout probabilities for the convolutional and fully connected layers. For FedL1, we considered a variety of regularization strengths. For each of these, we report the setting that performs best in terms of accuracy / communication trade-off.

The first task we consider is a federated version of CIFAR10 classification where we partition the data among 100 shards in a non-i.i.d. way following [12] and train a LeNet-5 convolutional architecture [17] for 1k rounds. For the second task, we consider the 500 shard federated version of CIFAR100 classification from [28], with a ResNet20 which we optimize for 6k rounds. For the final task, we considered the non-i.i.d. Femnist classification and we use the same configuration as CIFAR10, but we optimize the model for 6k rounds. More details can be found in Appendix A.

We evaluate FedSparse and the baselines on two metrics that highlight the tradeoffs between accuracy and communication costs. On both metrics, the x-axis represents the total communication cost incurred up until that point, and the y-axis represents two distinct model accuracies. The first one corresponds to the accuracy of the global model on the union of the shard test sets, whereas the second one corresponds to the average accuracy of the shard-specific “local models” on the shard-specific test sets. The “local model” on each shard is the model configuration that the shard last communicated to the server and serves as a proxy for the personalized model performance on each shard. The latter metric is motivated from the meta-learning [13] and hierarchical model view of federated learning and corresponds to using the local posteriors for prediction on the local test set instead of the server-side priors. All experiments were implemented using PyTorch [26].

5.1 Experimental results

The results from our experiments can be found in the following table and figures, where we report the average metrics and standard errors of each from 3 different random seeds. Overall, we observed that the FedSparse models achieve their final sparsity ratios early in training, *i.e.*, after 30-50 rounds, which quickly reduces the communication costs for each round (Appendix B).

Table 1: Cifar10

Method	Global acc.	Local acc.	GB comm.	Sparsity
FedAvg	69.7 \pm 0.3	86.2 \pm 0.2	65 \pm 0	-
FedDrop	69.9 \pm 0.7	84.9 \pm 0.2	34 \pm 0	-
FedL1	62.1 \pm 0.8	82.5 \pm 0.3	36 \pm 1	61.8 \pm 1.8
FedSparse, low	68.9 \pm 0.5	86.9 \pm 0.4	52 \pm 0	21.4 \pm 0.4
FedSparse, mid	68.9 \pm 0.4	87.6 \pm 0.1	35 \pm 0	46.8 \pm 0.4
FedSparse, high	68.4 \pm 0.5	86.9 \pm 0.2	23 \pm 1	66.5 \pm 0.8

Table 2: Cifar100

Method	Global acc.	Local acc.	GB comm.	Sparsity
FedAvg	40.6 \pm 1.0	61.5 \pm 0.6	124 \pm 0	-
FedDrop	36.1 \pm 0.5	57.8 \pm 0.3	112 \pm 0	-
FedL1	23.6 \pm 0.7	45.8 \pm 0.3	118 \pm 1	8.0 \pm 1.0
FedSparse, low	40.5 \pm 0.7	61.8 \pm 0.4	121 \pm 0	1.6 \pm 0.1
FedSparse, mid	31.7 \pm 1.0	54.8 \pm 0.6	58 \pm 1	53.8 \pm 0.6
FedSparse, high	23.8 \pm 2.0	48.5 \pm 1.5	43 \pm 2	66.9 \pm 1.3

Table 3: Femnist

Method	Global acc.	Local acc.	GB comm.	Sparsity
FedAvg	85.8 \pm 0.2	90.8 \pm 0.0	272 \pm 0	-
FedDrop	84.7 \pm 0.2	87.6 \pm 0.0	168 \pm 0	-
FedL1	82.0 \pm 0.3	85.9 \pm 0.0	187 \pm 2	45.5 \pm 1.2
FedSparse, low	85.4 \pm 0.2	90.8 \pm 0.0	270 \pm 0	1.0 \pm 0.2
FedSparse, mid	85.1 \pm 0.3	90.6 \pm 0.0	148 \pm 2	45.6 \pm 0.7
FedSparse, high	84.1 \pm 0.4	89.6 \pm 0.1	102 \pm 3	62.8 \pm 1.1

We can see that for CIFAR 10, the FedSparse models with medium (\sim 47%) and high (\sim 66%) sparsity outperform all other methods for small communications budgets on the global accuracy front but are eventually surpassed by FedDrop on higher budgets. However, on the local accuracy front, we see that the FedSparse models perform better than both baselines, achieving, *e.g.*, \sim 87% local accuracy with \sim 34% less communication compared to FedAvg. Overall, judging the final performance only, we see that FedDrop reaches the best accuracy on the global model, but FedSparse reaches the best accuracy in the local models. FedL1 was able to learn a sparse model that was comparable in size to the FedSparse ‘high’ setting, however, the final accuracies, both the global and the local, were worse than all of the other methods.

On CIFAR 100, the differences are less pronounced, as the models did not fully converge for the maximum number of rounds we use. Nevertheless, we still observe similar patterns; for small

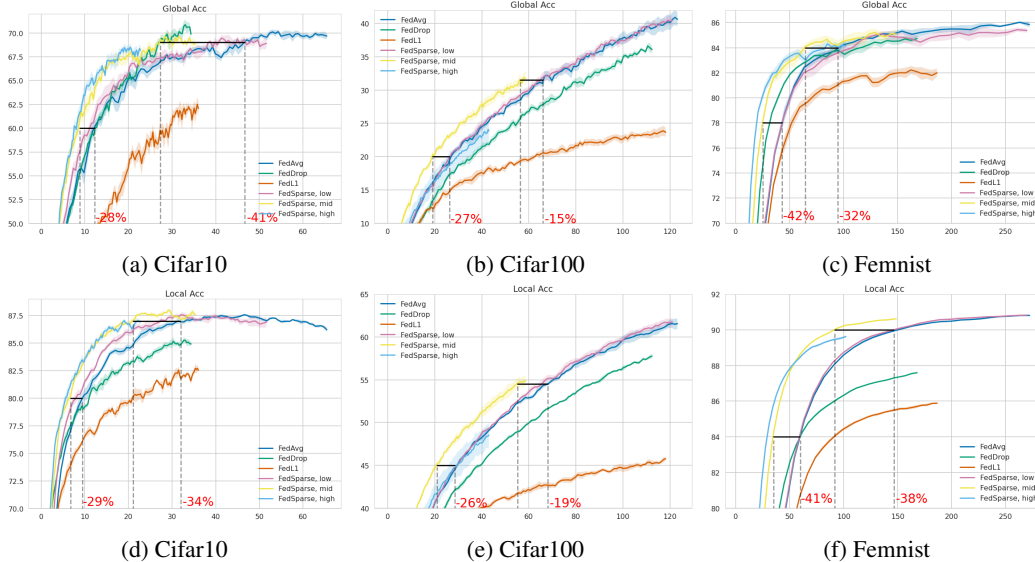


Figure 3: Global model accuracy (top row) and average local model accuracy (bottom row) across all clients (y-axis) as a function of the amount of GB communicated (top row). Best viewed in color.

communication budgets, the sparser models are better for both the global and local accuracy as, *e.g.*, they can reach $\sim 32\%$ global accuracy while requiring $\sim 15\%$ less communication than FedAvg.

Finally, for the FEMNIST task, which is also the more communication-intensive due to having $\sim 3.5k$ shards, we see that the FedSparse algorithm improves upon both FedDrop and FedAvg. More specifically, in the medium sparsification setting, it can reach $\sim 85\%$ global accuracy and $\sim 90\%$ local accuracy while requiring $\sim 32\%$ and $\sim 38\%$ less communication compared to FedAvg respectively. Judging by the final accuracy, both FedAvg and FedSparse with the low setting reached similar global and local model performance. This is expected, given that that particular FedSparse setting leads to only 1% sparsity. FedL1 did not outperform any of the other methods in terms of the final accuracies.

6 Conclusion

In this work, we adopted an interpretation of server-orchestrated federated learning as a hierarchical model where the server provides the parameters of a prior distribution over the parameters of client-specific models. We then showed how the FedAvg algorithm, the standard in federated learning, corresponds to applying the hard-EM algorithm to a hierarchical model that uses Gaussian priors. Through this perspective, we bridged several recent works on federated learning as well as connect FedAvg to meta-learning. As a straightforward extension stemming from this view, we proposed a hierarchical model with sparsity-inducing priors. By applying hard-EM on this new model, we obtained FedSparse, a generalization of FedAvg that can learn sparse neural networks in the federated learning setting. Empirically, we showed that FedSparse can learn sparse neural networks, which, besides being more efficient, can also significantly reduce the communication costs without decreasing performance - both of which are of great practical importance in “cross-device” federated learning. Of equal practical importance is hyperparameter resilience. In training models with FedSparse we observed a high sensitivity to hyperparameters related to initial sparsity thresholds and the necessity to downscale cross-entropy terms as discussed in Appendix A. A successful application of FedSparse therefore relies on careful tuning and provides ample opportunity for improvement in future work.

References

- [1] Maruan Al-Shedivat, Jennifer Gillenwater, Eric Xing, and Afshin Rostamizadeh. Federated learning via posterior averaging: A new perspective and practical algorithms. *arXiv preprint*

- arXiv:2010.05273*, 2020.
- [2] Mohammad Mohammadi Amiri, Deniz Gunduz, Sanjeev R Kulkarni, and H Vincent Poor. Federated learning with quantized global model updates. *arXiv preprint arXiv:2006.10672*, 2020.
 - [3] Kambiz Azarian, Yash Bhalgat, Jinwon Lee, and Tijmen Blankevoort. Learned threshold pruning. *arXiv preprint arXiv:2003.00075*, 2020.
 - [4] Jeremy Bernstein, Yu-Xiang Wang, Kamyar Azizzadenesheli, and Anima Anandkumar. signsgd: Compressed optimisation for non-convex problems. *arXiv preprint arXiv:1802.04434*, 2018.
 - [5] Sebastian Caldas, Jakub Konečný, H Brendan McMahan, and Ameet Talwalkar. Expanding the reach of federated learning by reducing client resource requirements. *arXiv preprint arXiv:1812.07210*, 2018.
 - [6] Yutian Chen, Abram L Friesen, Feryal Behbahani, David Budden, Matthew W Hoffman, Arnaud Doucet, and Nando de Freitas. Modular meta-learning with shrinkage. *arXiv preprint arXiv:1909.05557*, 2019.
 - [7] Luca Corinzia, Ami Beuret, and Joachim M Buhmann. Variational federated multi-task learning. *arXiv preprint arXiv:1906.06268*, 2019.
 - [8] Alireza Fallah, Aryan Mokhtari, and Asuman Ozdaglar. Personalized federated learning: A meta-learning approach. *arXiv preprint arXiv:2002.07948*, 2020.
 - [9] Trevor Gale, Erich Elsen, and Sara Hooker. The state of sparsity in deep neural networks. *arXiv preprint arXiv:1902.09574*, 2019.
 - [10] Erin Grant, Chelsea Finn, Sergey Levine, Trevor Darrell, and Thomas Griffiths. Recasting gradient-based meta-learning as hierarchical bayes. *arXiv preprint arXiv:1801.08930*, 2018.
 - [11] Pengchao Han, Shiqiang Wang, and Kin K Leung. Adaptive gradient sparsification for efficient federated learning: An online learning approach. *arXiv preprint arXiv:2001.04756*, 2020.
 - [12] Tzu-Ming Harry Hsu, Hang Qi, and Matthew Brown. Measuring the effects of non-identical data distribution for federated visual classification. *arXiv preprint arXiv:1909.06335*, 2019.
 - [13] Yihan Jiang, Jakub Konečný, Keith Rush, and Sreeram Kannan. Improving federated learning personalization via model agnostic meta learning. *arXiv preprint arXiv:1909.12488*, 2019.
 - [14] Peter Kairouz, H Brendan McMahan, Brendan Avent, Aurélien Bellet, Mehdi Bennis, Arjun Nitin Bhagoji, Keith Bonawitz, Zachary Charles, Graham Cormode, Rachel Cummings, et al. Advances and open problems in federated learning. *arXiv preprint arXiv:1912.04977*, 2019.
 - [15] Sai Praneeth Karimireddy, Satyen Kale, Mehryar Mohri, Sashank Reddi, Sebastian Stich, and Ananda Theertha Suresh. Scaffold: Stochastic controlled averaging for federated learning. In *International Conference on Machine Learning*, pages 5132–5143. PMLR, 2020.
 - [16] Diederik P Kingma and Jimmy Ba. Adam: A method for stochastic optimization. *arXiv preprint arXiv:1412.6980*, 2014.
 - [17] Yann LeCun, Léon Bottou, Yoshua Bengio, and Patrick Haffner. Gradient-based learning applied to document recognition. *Proceedings of the IEEE*, 86(11):2278–2324, 1998.
 - [18] Tian Li, Anit Kumar Sahu, Manzil Zaheer, Maziar Sanjabi, Ameet Talwalkar, and Virginia Smith. Federated optimization in heterogeneous networks. *arXiv preprint arXiv:1812.06127*, 2018.
 - [19] Zhize Li, Hongyan Bao, Xiangliang Zhang, and Peter Richtárik. Page: A simple and optimal probabilistic gradient estimator for nonconvex optimization. *arXiv preprint arXiv:2008.10898*, 2020.
 - [20] Yujun Lin, Song Han, Huizi Mao, Yu Wang, and William J Dally. Deep gradient compression: Reducing the communication bandwidth for distributed training. *arXiv preprint arXiv:1712.01887*, 2017.
 - [21] Christos Louizos, Max Welling, and Diederik P Kingma. Learning sparse neural networks through l_0 regularization. *arXiv preprint arXiv:1712.01312*, 2017.

- [22] H Brendan McMahan, Eider Moore, Daniel Ramage, Seth Hampson, et al. Communication-efficient learning of deep networks from decentralized data. *arXiv preprint arXiv:1602.05629*, 2016.
- [23] Toby J Mitchell and John J Beauchamp. Bayesian variable selection in linear regression. *Journal of the american statistical association*, 83(404):1023–1032, 1988.
- [24] Radford M Neal and Geoffrey E Hinton. A view of the em algorithm that justifies incremental, sparse, and other variants. In *Learning in graphical models*, pages 355–368. Springer, 1998.
- [25] Alex Nichol, Joshua Achiam, and John Schulman. On first-order meta-learning algorithms. *arXiv preprint arXiv:1803.02999*, 2018.
- [26] Adam Paszke, Sam Gross, Francisco Massa, Adam Lerer, James Bradbury, Gregory Chanan, Trevor Killeen, Zeming Lin, Natalia Gimelshein, Luca Antiga, Alban Desmaison, Andreas Kopf, Edward Yang, Zachary DeVito, Martin Raison, Alykhan Tejani, Sasank Chilamkurthy, Benoit Steiner, Lu Fang, Junjie Bai, and Soumith Chintala. Pytorch: An imperative style, high-performance deep learning library. In H. Wallach, H. Larochelle, A. Beygelzimer, F. d'Alché-Buc, E. Fox, and R. Garnett, editors, *Advances in Neural Information Processing Systems 32*, pages 8024–8035. Curran Associates, Inc., 2019.
- [27] Fabrizio Pittorino, Carlo Lucibello, Christoph Feinauer, Enrico M Malatesta, Gabriele Perugini, Carlo Baldassi, Matteo Negri, Elizaveta Demyanenko, and Riccardo Zecchina. Entropic gradient descent algorithms and wide flat minima. *arXiv preprint arXiv:2006.07897*, 2020.
- [28] Sashank Reddi, Zachary Charles, Manzil Zaheer, Zachary Garrett, Keith Rush, Jakub Konečný, Sanjiv Kumar, and H Brendan McMahan. Adaptive federated optimization. *arXiv preprint arXiv:2003.00295*, 2020.
- [29] Reginaldo J Santos. Equivalence of regularization and truncated iteration for general ill-posed problems. *Linear algebra and its applications*, 236:25–33, 1996.
- [30] Felix Sattler, Simon Wiedemann, Klaus-Robert Müller, and Wojciech Samek. Robust and communication-efficient federated learning from non-iid data. *IEEE transactions on neural networks and learning systems*, 2019.
- [31] Jianqiao Wangni, Jialei Wang, Ji Liu, and Tong Zhang. Gradient sparsification for communication-efficient distributed optimization. In *Advances in Neural Information Processing Systems*, pages 1299–1309, 2018.
- [32] Wei Wen, Chunpeng Wu, Yandan Wang, Yiran Chen, and Hai Li. Learning structured sparsity in deep neural networks. *arXiv preprint arXiv:1608.03665*, 2016.
- [33] Yue Yu, Jiayang Wu, and Longbo Huang. Double quantization for communication-efficient distributed optimization. In *Advances in Neural Information Processing Systems*, pages 4438–4449, 2019.
- [34] Mikhail Yurochkin, Mayank Agarwal, Soumya Ghosh, Kristjan Greenewald, Nghia Hoang, and Yasaman Khazaeni. Bayesian nonparametric federated learning of neural networks. In *International Conference on Machine Learning*, pages 7252–7261. PMLR, 2019.
- [35] Mikhail Yurochkin, Mayank Agarwal, Soumya Ghosh, Kristjan Greenewald, and Trong Nghia Hoang. Statistical model aggregation via parameter matching. *arXiv preprint arXiv:1911.00218*, 2019.
- [36] Michael Zhang, James Lucas, Jimmy Ba, and Geoffrey E Hinton. Lookahead optimizer: k steps forward, 1 step back. In *Advances in Neural Information Processing Systems*, pages 9597–9608, 2019.

A Experimental details

For all of the three tasks we randomly select 10 clients without replacement in a given round but with replacement across rounds. For the local optimizer of the weights we use stochastic gradient descent with a learning rate of 0.05, whereas for the global optimizer we use Adam [16] with the default hyperparameters provided in [16]. For the pruning thresholds in FedSparse we used the Adamax [16] optimizer with $1e - 3$ learning rate at the shard level and the Adamax optimizer with $1e - 2$ learning rate at the server. For all three of the tasks we used $E = 1$ with a batch size of 64

for CIFAR10 and 20 for CIFAR100 and Femnist. It should be noted that for all the methods we performed gradient based optimization using the difference gradient for the weights [28] instead of averaging.

For the FedDrop baseline, we used a very small dropout rate of 0.01 for the input and output layer and tuned the dropout rates for convolutional and fully connected layers separately in order to optimize the accuracy / communication tradeoff. For convolutional layers we considered rates in $\{0.1, 0.2, 0.3\}$ whereas for the fully connected layers we considered rates in $\{0.1, 0.2, 0.3, 0.4, 0.5\}$. For CIFAR10 we did not employ the additional dropout noise at the shard level, since we found that it was detrimental for the FedDrop performance. Furthermore, for Resnet20 on CIFAR100 we did not apply federated dropout at the output layer. For CIFAR10 the best performing dropout rates were 0.1 for the convolutional and 0.5 for the fully connected, whereas for CIFAR100 it was 0.1 for the convolutional. For Femnist, we saw that a rate of 0.2 for the convolutional and a rate of 0.4 for the fully connected performed better.

For FedSparse, we initialized \mathbf{v} such that the thresholds τ lead to $\theta = 0.99$ initially, *i.e.* we started from a dense model. The temperature for the sigmoid in the parameterization of the probabilities was set to $T = 0.001$. Furthermore, we downscaled the cross-entropy term between the client side probabilities, π_s , and the server side probabilities, θ by multiplying it with $1e - 4$. Since at the beginning of each round we were always initializing $\pi_s = \theta$ and we were only optimizing for a small number of steps before synchronizing, we found that the full strength of the cross-entropy was not necessary. Furthermore, for similar reasons, *i.e.* we set $\mathbf{w}_s = \mathbf{w}$ at the beginning of each round, we also used $\lambda = 0$ for the drift term $\frac{\lambda}{2} \pi_{sj} (\mathbf{w}_s - \mathbf{w})^2$. The remaining hyperparameter λ_0 dictates how sparse the final model will be. For the LeNet-5 model the λ_0 's we report are $\{5e - 7, 5e - 6, 5e - 5\}$ for the “low”, “mid” and “high” settings respectively, which were optimized for CIFAR10 and used as-is for Femnist. For CIFAR100 and Resnet20, we did not perform any pruning for the output layer and the λ_0 's for the “low”, “mid” and “high” settings were $\{5e - 7, 5e - 6, 5e - 5\}$ respectively. These were chosen so that we obtain models with comparable sparsity ratios as the one on CIFAR10.

The FedL1 baseline was implemented by using a group L_1 regularizer [32] at the client level, *i.e.*, the local loss was:

$$\mathcal{L}_s(\mathcal{D}_s, \mathbf{w}) := \frac{1}{N_s} \sum_{i=1}^{N_s} L(\mathcal{D}_{si}, \mathbf{w}) + \lambda \sum_g \sqrt{\|\mathbf{w}_g\|_2^2}, \quad (24)$$

where \mathbf{w}_g was the vector of parameters associated with group g . To have similar sparsity patterns to FedSparse, each of the groups of parameters were chosen to be the weights associated with a specific neuron (in case of a fully connected layer) or a specific feature map (in case of a convolutional layer). In order to realize the sparse communication, we employed a thresholding operator before each client and the server communicated their parameters:

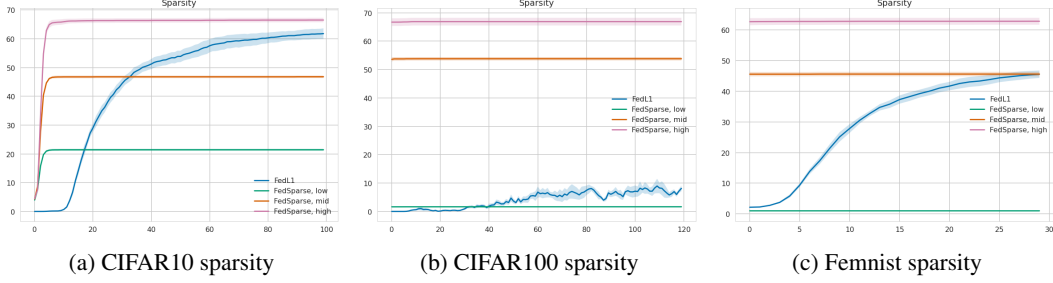
$$\hat{\mathbf{w}}_g = \mathbf{w}_g z_g, \quad z_g = \begin{cases} 0, & \text{if } \sqrt{\|\mathbf{w}_g\|_2^2} \leq \lambda \\ 1, & \text{otherwise} \end{cases} \quad (25)$$

We empirically found that this operator resulted into better overall model performance, compared to the more traditional soft-thresholding one, which also “shrinks” the non-pruned parameters. The server used the traditional parameter difference between the communicated, sparse, local model and the current server model for gradient based optimization. To obtain the results in the main text, we used $\lambda = 2e - 3$ for CIFAR10 and CIFAR100, whereas for Femnist we used $\lambda = 1e - 3$. These values were chosen so that we obtain comparable sparsities to the ones from FedSparse.

Most of the experiments were run on an Nvidia RTX 2080Ti GPU, and the hyperparameter optimization was performed with several Nvidia V100 GPU's on an internal cluster over the span of a month.

B Evolution of sparsity

We show the evolution of the sparsity ratios for all tasks and configurations in the following plot. We can see that in all settings the model attains its final sparsity quite early in training (*i.e.*, before 100 rounds) in the case of FedSparse whereas with FedL1 the sparsity is achieved much later in training. As a result, the communication savings (of the overall training procedure) with FedL1 are not as much as the ones from FedSparse.



C Sparsity alignment between clients and server

A reasonable question to ask is whether the local sparsity patterns between clients “align”; if the clients do not agree on which parameters to prune, the server model will not be sparse and therefore we won’t get as much communication cost benefit. To test where such an issue happens in practice with FedSparse we implemented two metrics that track the average and maximum total variation distance between the gating distributions (*i.e.*, those that control the sparsity patterns) of the clients and the server. The total variation distance corresponds to the absolute difference between the client and server probabilities for the binary gates, *i.e.*,

$$\text{TV}(q_{\pi_s}(z_s), p_{\theta}(z_s)) = |q_{\pi_s}(z_s = 1) - p_{\theta}(z_s = 1)| = |\pi_s - \theta| \quad (26)$$

The resulting plots over the course of training for all tasks and FedSparse settings can be found in Fig. 5. We can clearly see that the clients and the server quickly agree on the general sparsity pattern

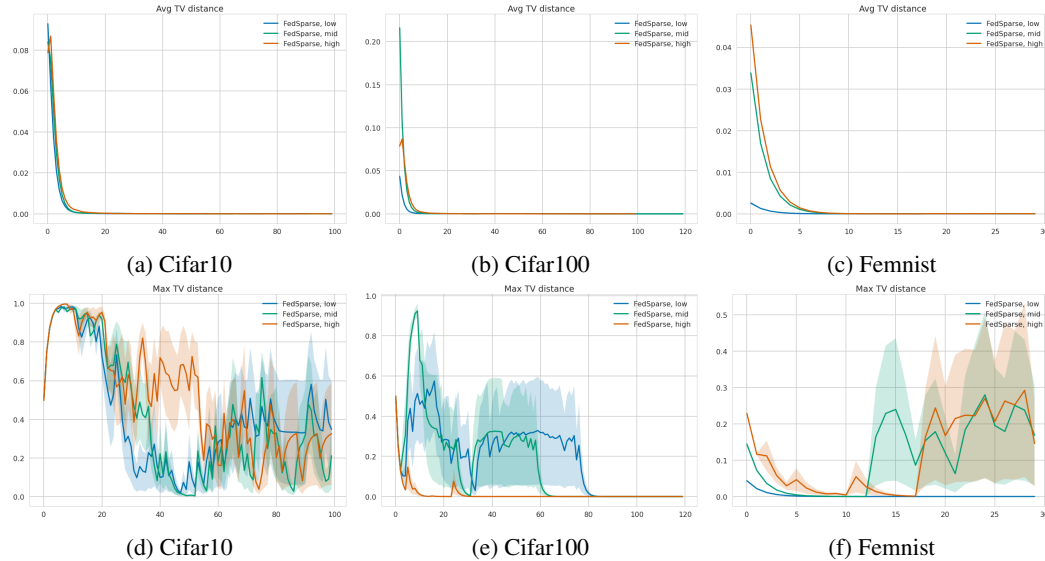


Figure 5: Average (top row) and maximum (bottom row) total variation distance for all tasks and FedSparse settings.

as the average total variation distance becomes almost zero on all settings. We can attribute this to the “resetting” of the local $q_{\pi_s}(z_s)$ to $p_{\theta}(z_s)$ configuration that happens at the beginning of each round along with the extra cross-entropy loss between $q_{\pi_s}(z_s), p_{\theta}(z_s)$ that FedSparse has. We can also see that the maximum total variation distance takes much longer to drop, meaning that there are a few parameter groups where the probability of keeping them at the clients’ sides is different than the one at the server. We attribute this to the model “specializing” the sparsity pattern to the characteristics of the client dataset. We can also see however, that the maximum total variation distance does drop as training progresses, showing that the sparsity pattern specialization does decrease (although it never becomes zero).

D Additional results

Convergence plots in terms of communication rounds. In order to understand whether the extra noise is detrimental to the convergence speed of FedSparse, we plot the validation accuracy in terms of communication rounds for all tasks and baselines. As it can be seen, there is no inherent difference before FedSparse starts pruning. This happens quite early in training for CIFAR 100 thus it is there where we observe the most differences. FedL1 is overall worse than the other methods as the inclusion of the L_1 penalty hurts model performance.

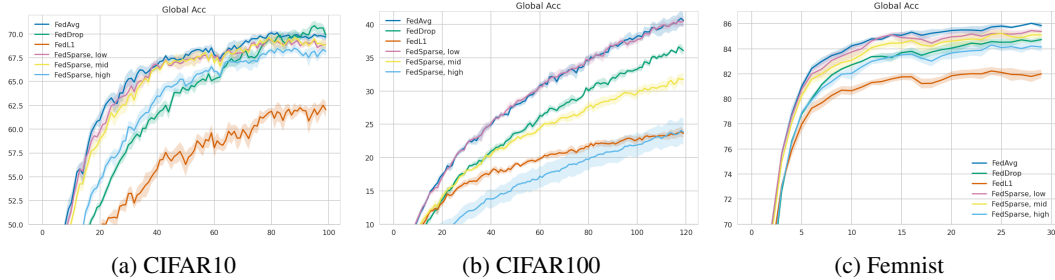


Figure 6: Evolution of the validation accuracy in terms of communication rounds.

Impact of server side pruning. In order to understand whether server side pruning is harmful for convergence, we plot both the global and average local validation accuracy on CIFAR 10 for the “mid” setting of FedSparse with and without server side pruning enabled. As we can see, there are no noticeable differences and in fact, pruning results into a slightly better overall performance.

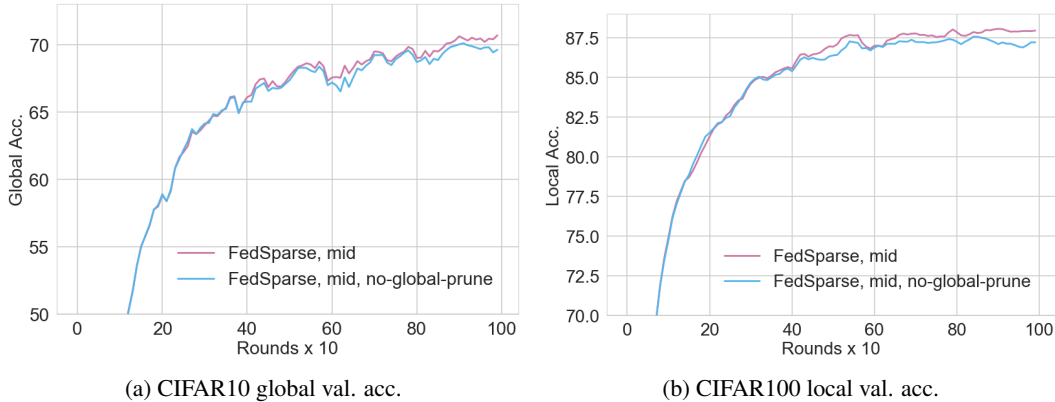


Figure 7: Evolution of the validation accuracy in terms of communication rounds with and without server side pruning.

E Combining SCAFFOLD with FedSparse

In order to show that techniques such as [15, 19] are orthogonal to FedSparse, we implement SCAFFOLD [15] on a simple convex problem (following their theory); logistic regression on a (extreme) non-iid split of the MNIST dataset into 100 users (each user had data from a single class) trained for 400 rounds. For the combination of FedSparse and SCAFFOLD, we used the SCAFFOLD procedure for the weights. The results can be seen in Figure 8.

When measuring the global model accuracy, we observe the benefits of SCAFFOLD compared to FedAvg. Nevertheless, the “local model“ accuracy (as defined in the main text) was worse, probably due to the control variates leading to a model that is less fine-tuned on the local data-sets. By comparing these results to the ones with FedSparse, we can see that indeed FedSparse is orthogonal to SCAFFOLD, so one can combine both methods to get the best of both worlds. The model sparsity

for FedSparse was around 35% when including SCAFFOLD and 47% without. It should be noted that SCAFFOLD doubles the communication cost per round (compared to FedAvg) due to transmitting the control variates.

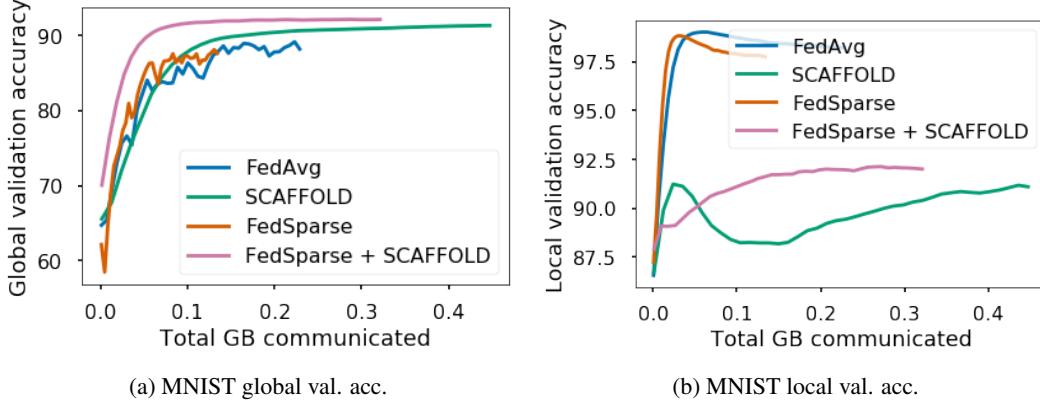


Figure 8: Evolution of the validation accuracy in terms of the GB communicated for FedAvg, SCAFFOLD, FedSparse and FedSparse with SCAFFOLD.

On the neural network architectures of the main text, the picture was not as clear since SCAFFOLD lead to unstable optimization, which only stabilised after we "dampened" the contribution from the control variates to the local training procedure (thus not providing benefits). Since in [15] it is mentioned that on non-convex problems "much more extensive experiments (beyond current scope) are needed before drawing conclusions", we did not pursue this further.

F Correspondence between single step EM and gradient ascent

With the addition of the auxiliary variables ϕ_s we have that the overall objective for the server becomes

$$\arg \max_{\mathbf{w}} \frac{1}{S} \sum_{s=1}^S \log \int p(\mathcal{D}_s | \phi_s) p(\phi_s | \mathbf{w}) d\phi_s. \quad (27)$$

By performing EM with a single gradient step for \mathbf{w} in the M-step (instead of full maximization), we are essentially doing gradient ascent on the original objective at 27. To see this, we can take the gradient of Eq. 27 w.r.t. \mathbf{w} where $Z_s = \int p(\mathcal{D}_s | \phi_s) p(\phi_s | \mathbf{w}) d\phi_s$

$$\frac{1}{S} \sum_s \frac{1}{Z_s} \int p(\mathcal{D}_s | \phi_s) \frac{\partial p(\phi_s | \mathbf{w})}{\partial \mathbf{w}} d\phi_s = \quad (28)$$

$$\frac{1}{S} \sum_s \int \frac{p(\mathcal{D}_s | \phi_s) p(\phi_s | \mathbf{w})}{Z_s} \frac{\partial \log p(\phi_s | \mathbf{w})}{\partial \mathbf{w}} d\phi_s = \quad (29)$$

$$\frac{1}{S} \sum_s \int p(\phi_s | \mathcal{D}_s, \mathbf{w}) \frac{\partial \log p(\phi_s | \mathbf{w})}{\partial \mathbf{w}} d\phi_s \quad (30)$$

where to compute Eq. 30 we see that we first have to obtain the posterior distribution of the local variables ϕ_s and then estimate the gradient for \mathbf{w} by marginalizing over this posterior.

G Derivation of the local loss for FedSparse

Let $p(\phi_{si} | \mathbf{w}_i, \mathbf{z}_{si} = 1) = \mathcal{N}(\mathbf{w}_i, 1/\lambda)$, $p(\phi_{si} | \mathbf{w}_i, \mathbf{z}_{si} = 0) = \mathcal{N}(0, 1/\lambda_2)$ and $q(\phi_{si} | \mathbf{z}_{si} = 1) = \mathcal{N}(\mathbf{w}_{si}, \epsilon^2)$, $q(\phi_{si} | \mathbf{z}_{si} = 0) = \mathcal{N}(0, \epsilon^2)$. Furthermore, let $q(\mathbf{z}_{si}) = \text{Bern}(\pi_{si})$. The local objective that stems from 16 can be rewritten as:

$$\begin{aligned} \arg \max_{\mathbf{w}_{1:S}, \pi_{1:S}} \mathbb{E}_{q_{\pi_s}(\mathbf{z}_s) q_{\mathbf{w}_s}(\phi_s | \mathbf{z}_s)} [\log p(\mathcal{D}_s | \phi_s)] - \mathbb{E}_{q_{\pi_s}(\mathbf{z}_s)} [KL(q_{\mathbf{w}_s}(\phi_s | \mathbf{z}_s) || p(\phi_s | \mathbf{w}, \mathbf{z}_s))] \\ + \mathbb{E}_{q_{\pi_s}(\mathbf{z}_s)} [\log p(\mathbf{z}_s | \boldsymbol{\theta})], \end{aligned} \quad (31)$$

where we omitted from the objective the entropy of the distribution over the local gates.

One of the quantities that we are after is

$$\mathbb{E}_{q(\mathbf{z}_{si})}[KL(q(\phi_{si}|\mathbf{z}_{si})||p(\phi_{si}|\mathbf{z}_{si}))] = \pi_{si}KL(\mathcal{N}(\mathbf{w}_{si}, \epsilon^2)||\mathcal{N}(\mathbf{w}_i, 1/\lambda)) + (1 - \pi_{si})KL(\mathcal{N}(0, \epsilon^2)||\mathcal{N}(0, 1/\lambda_2)). \quad (32)$$

The KL term for when $\mathbf{z}_{si} = 1$ can be written as

$$KL(\mathcal{N}(\mathbf{w}_{si}, \epsilon^2)||\mathcal{N}(\mathbf{w}_i, 1/\lambda)) = -\frac{1}{2}\log \lambda - \log \epsilon + \frac{\lambda\epsilon^2}{2} - \frac{1}{2} + \frac{\lambda}{2}(\mathbf{w}_{si} - \mathbf{w}_i)^2. \quad (33)$$

The KL term for when $\mathbf{z}_{si} = 0$ can be written as

$$KL(\mathcal{N}(0, \epsilon^2)||\mathcal{N}(0, 1/\lambda_2)) = -\frac{1}{2}\log \lambda_2 - \log \epsilon + \frac{\lambda_2\epsilon^2}{2} - \frac{1}{2}. \quad (34)$$

Taking everything together we thus have

$$\begin{aligned} \mathbb{E}_{q(\mathbf{z}_{si})}[KL(q(\phi_{si}|\mathbf{z}_{si})||p(\phi_{si}|\mathbf{z}_{si}))] &= \frac{\lambda\pi_{si}}{2}(\mathbf{w}_{si} - \mathbf{w}_i)^2 + \pi_{si}\left(-\frac{1}{2}\log \lambda - \log \epsilon + \frac{\lambda\epsilon^2}{2} - \frac{1}{2}\right) + \\ &\quad (1 - \pi_{si})\left(-\frac{1}{2}\log \lambda_2 - \log \epsilon + \frac{\lambda_2\epsilon^2}{2} - \frac{1}{2}\right) \end{aligned} \quad (35)$$

$$= \frac{\lambda\pi_{si}}{2}(\mathbf{w}_{si} - \mathbf{w}_i)^2 + \pi_{si}\left(\frac{1}{2}\log \frac{\lambda_2}{\lambda} + \frac{\epsilon^2}{2}(\lambda - \lambda_2)\right) + C \quad (36)$$

$$\approx \frac{\lambda\pi_{si}}{2}(\mathbf{w}_{si} - \mathbf{w}_i)^2 + \lambda_0\pi_{si} + C, \quad (37)$$

where $\lambda_0 = \frac{1}{2}\log \frac{\lambda_2}{\lambda}$ and $\frac{\epsilon^2}{2}(\lambda - \lambda_2)$ was omitted due to $\epsilon^2 \approx 0$. In the appendix of [21], the authors argue about a hypothetical prior that results into needing λ nats to transform that prior to the approximate posterior. Here we make this claim more precise and show that this prior is approximately equivalent to a mixture of Gaussians prior where the precision of the non-zero prior component $\lambda \rightarrow \epsilon$ (in order to avoid the L_2 regularization term) and the precision of the zeroth component λ_2 is equivalent to $\lambda \exp(2\lambda_0)$, where λ_0 is the desired L_0 regularization strength.

Furthermore, the cross-entropy from $q_{\pi_s}(\mathbf{z}_s)$ to $p(\mathbf{z}_s|\boldsymbol{\theta})$ is straightforward to compute as

$$\mathbb{E}_{q_{\pi_s}(\mathbf{z}_s)}[\log p(\mathbf{z}_s|\boldsymbol{\theta})] = \sum_j (\pi_{sj} \log \theta_j + (1 - \pi_{sj}) \log(1 - \theta_j)). \quad (38)$$

By putting everything together we have that the local objective becomes

$$\begin{aligned} \arg \max_{\mathbf{w}_s, \pi_s} \mathbb{E}_{q_{\pi_s}(\mathbf{z}_s)} \left[\sum_i^{N_s} L(\mathcal{D}_{si}, \mathbf{w}_s \odot \mathbf{z}_s) \right] &- \frac{\lambda}{2} \sum_j \pi_{sj} (\mathbf{w}_{sj} - \mathbf{w}_j)^2 - \lambda_0 \sum_j \pi_{sj} \\ &+ \sum_j (\pi_{sj} \log \theta_j + (1 - \pi_{sj}) \log(1 - \theta_j)) + C. \end{aligned} \quad (39)$$

H Local optimization of the binary gates

We propose to rewrite the local loss in Eq. 16 to

$$\begin{aligned} \mathcal{L}_s(\mathcal{D}_s, \mathbf{w}, \boldsymbol{\theta}, \phi_s, \pi_s) &:= \mathbb{E}_{q_{\pi_s}(\mathbf{z}_s)} \left[\sum_i^{N_s} L(\mathcal{D}_{si}, \mathbf{w}_s \odot \mathbf{z}_s) - \lambda \sum_j \mathbb{I}[\mathbf{z}_{sj} \neq 0] (\mathbf{w}_{sj} - \mathbf{w})^2 \right. \\ &\quad \left. - \lambda_0 \sum_j \mathbb{I}[\mathbf{z}_{sj} \neq 0] + \sum_j \left(\mathbb{I}[\mathbf{z}_{sj} \neq 0] \log \frac{\theta_j}{1 - \theta_j} + \log(1 - \theta_j) \right) \right], \end{aligned} \quad (40)$$

and then replace the Bernoulli distribution $q_{\pi_s}(\mathbf{z}_s)$ with a continuous relaxation, the hard-concrete distribution [21]. Let the continuous relaxation be $r_{\mathbf{u}_s}(\mathbf{z}_s)$, where \mathbf{u}_s are the parameters of the

surrogate distribution. In this case the local objective becomes

$$\begin{aligned} \mathcal{L}_s(\mathcal{D}_s, \mathbf{w}, \boldsymbol{\theta}, \boldsymbol{\phi}_s, \mathbf{u}_s) &:= \mathbb{E}_{r_{\mathbf{u}_s}(\mathbf{z}_s)} \left[\sum_i^{N_s} L(\mathcal{D}_{si}, \mathbf{w}_s \odot \mathbf{z}_s) \right] - \lambda \sum_j R_{\mathbf{u}_{sj}}(\mathbf{z}_{sj} > 0) (\mathbf{w}_{sj} - \mathbf{w})^2 \\ &\quad - \lambda_0 \sum_j R_{\mathbf{u}_{sj}}(\mathbf{z}_{sj} > 0) + \sum_j \left(R_{\mathbf{u}_{sj}}(\mathbf{z}_{sj} > 0) \log \frac{\boldsymbol{\theta}_j}{1 - \boldsymbol{\theta}_j} + \log(1 - \boldsymbol{\theta}_j) \right), \quad (41) \end{aligned}$$

where $R_{\mathbf{u}_s}(\cdot)$ is the cumulative distribution function (CDF) of the continuous relaxation $r_{\mathbf{u}_s}(\cdot)$. We can now straightforwardly optimize the surrogate objective with gradient ascent.

I FedSparse algorithm

Algorithm 1 The server side algorithm for FedSparse (assuming weight sparsity for simplicity). $\sigma(\cdot)$ is the sigmoid function, ϵ is the threshold for pruning.

```

Initialize  $\mathbf{v}$  and  $\mathbf{w}$ 
for round  $t$  in  $1, \dots, T$  do
   $\tau \leftarrow \log(1 + \exp(\mathbf{v}))$ 
   $\theta \leftarrow \sigma((|\mathbf{w}| - \tau)/T)$ 
   $\mathbf{w} \leftarrow \mathbb{I}[\theta > \epsilon]\mathbf{w}$  ▷ prune global model
  Initialize  $\nabla_{\mathbf{w}}^t = \mathbf{0}, \nabla_{\mathbf{v}}^t = \mathbf{0}$ 
  for  $s$  in random subset of the clients do
     $\mathbf{z}_s, \hat{\mathbf{w}}_s^t \leftarrow \text{CLIENT}(s, \mathbf{w}, \mathbf{v})$ 
     $\nabla_{\mathbf{w}}^t \leftarrow \nabla_{\mathbf{w}}^t + \mathbf{z}_s(\hat{\mathbf{w}}_s^t - \mathbf{w})$ 
     $\nabla_{\mathbf{v}}^t \leftarrow \nabla_{\mathbf{v}}^t - (\mathbf{z}_s(1 - \theta) - (1 - \mathbf{z}_s)\theta) \sigma(\mathbf{v})/T$ 
  end for
   $\mathbf{w}^{t+1}, \mathbf{v}^{t+1} \leftarrow \text{ADAM}(\nabla_{\mathbf{w}}^t), \text{ADAMAX}(\nabla_{\mathbf{v}}^t)$ 
end for

```

Algorithm 2 The client side algorithm for FedSparse.

```

Get  $\mathbf{w}, \mathbf{v}$  from the server
 $\theta \leftarrow \sigma((|\mathbf{w}| - \tau)/T)$ 
 $\mathbf{w}_s, \mathbf{v}_s \leftarrow \mathbf{w}, \mathbf{v}$ 
for epoch  $e$  in  $1, \dots, E$  do
  for batch  $b \in B$  do
     $\tau_s \leftarrow \log(1 + \exp(\mathbf{v}_s))$ 
     $\pi_s \leftarrow \sigma((|\mathbf{w}_s| - \tau_s)/T)$ 
     $L_s \leftarrow \mathcal{L}_s(b, \mathbf{w}, \theta, \mathbf{w}_s, \pi_s)$ 
     $\mathbf{w}_s \leftarrow \text{SGD}(\nabla_{\mathbf{w}_s} L_s)$ 
     $\mathbf{v}_s \leftarrow \text{ADAMAX}(\nabla_{\mathbf{v}_s} L_s)$ 
  end for
end for
 $\pi_s \leftarrow \sigma((|\mathbf{w}_s| - \tau_s)/T)$ 
 $\mathbf{z}_s \sim q_{\pi_s}(\mathbf{z}_s)$ 
return  $\mathbf{z}_s, \mathbf{z}_s \odot \mathbf{w}_s$ 

```

J Alternative priors for the hierarchical model

In the main text we argued that the hierarchical model interpretation is highly flexible and allows for straightforward extensions. In this section we will demonstrate two variants that use either a Laplace or a mixture of Gaussians prior, coupled with hard-EM for learning the parameters of the hierarchical model.

J.1 Federated learning with Laplace priors

Lets start with the Laplace variant; the Laplace density for a specific local parameter ϕ_{si} will be:

$$p(\phi_{si} | \mathbf{w}_i) = \frac{\lambda}{2} \exp(-\lambda |\phi_{si} - \mathbf{w}_i|). \quad (42)$$

Therefore the local objective of each shard and the global objective will be

$$\mathcal{L}_s(\mathcal{D}_s, \mathbf{w}, \mathbf{w}_s) := \sum_i^{N_s} L(\mathcal{D}_{si}, \mathbf{w}_s) - \lambda \sum_j |\mathbf{w}_{sj} - \mathbf{w}_j| + C, \quad (43)$$

$$\mathcal{L}(\mathbf{w}) := \sum_s \mathcal{L}_s(\mathcal{D}_s, \mathbf{w}, \mathbf{w}_s) \quad (44)$$

where again the global objective is a sum of all the local objectives and C is a constant independent of the optimization. We can then proceed, in a similar fashion to traditional “cross-device” FL, by selecting a subset of shards B to approximate the global objective. On these specific shards, we will then optimize \mathcal{L}_s with respect to \mathbf{w}_s while keeping \mathbf{w} fixed. Interestingly, due to the L_1 regularization term that appears in the local objective, we will have, depending on the regularization strength λ , several local parameters \mathbf{w}_s that will be exactly equal to the server parameters \mathbf{w} even after optimization. Now given the optimized parameters from these shards, \mathbf{w}_s^* , we will update the server parameters \mathbf{w} for the M-step by either a gradient update or a closed form solution. Taking the derivative of the global objective with respect to a \mathbf{w}_j we see that it has the following simple form

$$\frac{\partial L}{\partial \mathbf{w}_j} = \lambda \sum_{s \in B} \text{sign}(\mathbf{w}_{sj} - \mathbf{w}_j). \quad (45)$$

By setting it to zero, we see that the closed form solution is again easy to obtain

$$\frac{\partial L}{\partial \mathbf{w}_j} = 0 \Rightarrow \lambda \sum_{s \in B} \text{sign}(\mathbf{w}_{sj} - \mathbf{w}_j) = 0 \Rightarrow \mathbf{w}_j = \text{median}(\mathbf{w}_{1j}, \dots, \mathbf{w}_{Bj}) \quad (46)$$

since the median produces an equal number of positive and negative signs. Using the median in the server for updating its parameters is interesting, as it is more robust to “outlier” updates from the clients.

J.2 Federated learning with mixture of Gaussian priors

The mixture of Gaussians prior will allow us to learn an ensemble of models at the server. The density for the entire vector of local parameters \mathbf{w}_s in the case of K equiprobable components in the mixture will be

$$p(\phi_s | \mathbf{w}_{1:K}) = \frac{1}{K} \sum_k \mathcal{N}(\mathbf{w}_k, (1/\lambda)\mathbf{I}). \quad (47)$$

This will lead to the following local and global objectives

$$\mathcal{L}_s(\mathcal{D}_s, \mathbf{w}_{1:K}, \mathbf{w}_s) := \sum_i^{N_s} L(\mathcal{D}_{si}, \mathbf{w}_s) + \log \sum_k \frac{Z_k}{K} \exp\left(-\frac{\lambda}{2} \|\mathbf{w}_s - \mathbf{w}_k\|^2\right), \quad (48)$$

$$\mathcal{L}(\mathbf{w}_{1:K}) := \sum_s \mathcal{L}_s(\mathcal{D}_s, \mathbf{w}_{1:K}, \mathbf{w}_s) \quad (49)$$

where Z_k is the normalizing constant of component k . Now we can proceed in a similar fashion and select a subset of shards B to obtain the ϕ_s^* while keeping the parameters of the prior $\mathbf{w}_{1:K}$ fixed. Now by taking the gradient with respect to one of the members of the ensemble \mathbf{w}_k , given the optimized local parameters ϕ_s^* , we see that

$$\frac{\partial L}{\partial \mathbf{w}_k} = \lambda \sum_s \frac{\frac{Z_k}{K} \exp(-\frac{\lambda}{2} \|\mathbf{w}_s - \mathbf{w}_k\|^2)}{\sum_j \frac{Z_j}{K} \exp(-\frac{\lambda}{2} \|\mathbf{w}_s - \mathbf{w}_j\|^2)} (\mathbf{w}_s - \mathbf{w}_k). \quad (50)$$

Notice that this gradient estimate can also be interpreted in terms of a posterior distribution over the index z (taking values in $\{1, \dots, K\}$) given the “observed” variables \mathbf{w}_s ; we can treat $1/K$ as the prior probability of selecting component $z = k$, i.e., $p(z = k)$ and $Z_k \exp(-\frac{\lambda}{2} \|\mathbf{w}_s - \mathbf{w}_k\|)$ as the probability of \mathbf{w}_s under Gaussian component k . In this way, the weighting term can be written as

$$\frac{\frac{Z_k}{K} \exp(-\frac{\lambda}{2} \|\mathbf{w}_s - \mathbf{w}_k\|^2)}{\sum_j \frac{Z_j}{K} \exp(-\frac{\lambda}{2} \|\mathbf{w}_s - \mathbf{w}_j\|^2)} = p(z = k | \mathbf{w}_s, \mathbf{w}_{1:K}, \lambda). \quad (51)$$

This makes apparent the connection to Gaussian mixture models, since $p(z = k | \mathbf{w}_s, \mathbf{w}_{1:K}, \lambda)$ is equivalent to the responsibility of component k generating \mathbf{w}_s . Now we can again find a closed form solution for \mathbf{w}_k by setting the derivative to zero

$$\frac{\partial L}{\partial \mathbf{w}_k} = 0 \Rightarrow \lambda \sum_s p(z = k | \mathbf{w}_s, \mathbf{w}_{1:K}, \lambda) (\mathbf{w}_s - \mathbf{w}_k) \Rightarrow \mathbf{w}_k = \sum_s \frac{p(z = k | \mathbf{w}_s, \mathbf{w}_{1:K}, \lambda)}{\sum_j p(z = k | \mathbf{w}_j, \mathbf{w}_{1:K}, \lambda)} \mathbf{w}_s, \quad (52)$$

which is again similar to the closed form update for the centroids in a Gaussian mixture model when trained with EM.